Proteasome-Mediated Turnover of Arabidopsis MED25 Is Coupled to the Activation of *FLOWERING LOCUS T* Transcription[1][W]

Sabrina Iñigo, Adrián N. Giraldez[2], Joanne Chory, and Pablo D. Cerdán*

Fundación Instituto Leloir, IIBBA-Consejo Nacional de Investigaciones Científicas y Técnicas, C1405BWE Buenos Aires, Argentina (S.I., A.N.G., P.D.C.); Facultad de Ciencias Exactas y Naturales, Universidad de Buenos Aires, C1428EGA Buenos Aires, Argentina (P.D.C.); Universidad Nacional de Quilmes, B1876BXD Bernal, Argentina (S.I.); and Howard Hughes Medical Institute and Plant Biology Laboratory, Salk Institute for Biological Studies, La Jolla, California 92037 (J.C.)

The Mediator complex is a greater than 1-megadalton complex, composed of about 30 subunits and found in most eukaryotes, whose main role is to transmit signals from DNA-bound transcription factors to RNA Polymerase II. The proteasome is emerging as an important regulator of transcription during both initiation and elongation. It is increasing the number of cases where the proteolysis of transcriptional activators by the proteasome activates their function. This counterintuitive phenomenon was called "activation by destruction." Here, we show that, in Arabidopsis (*Arabidopsis thaliana*), PHYTOCHROME AND FLOWERING TIME1 (PFT1), the MEDIATOR25 (MED25) subunit of the plant Mediator complex, is degraded by the proteasome and that proteasome-mediated PFT1 turnover is coupled to its role in stimulating the transcription of *FLOWERING LOCUS T*, the plant florigen, which is involved in the process of flowering induction. We further identify two novel RING-H2 proteins that target PFT1 for degradation. We show that MED25-BINDING RING-H2 PROTEIN1 (MBR1) and MBR2 bind to PFT1 in yeast (*Saccharomyces cerevisiae*) and in vitro, and they promote PFT1 degradation in vivo, in a RING-H2-dependent way, typical of E3 ubiquitin ligases. We further show that both MBR1 and MBR2 also promote flowering by PFT1-dependent and -independent mechanisms. Our findings extend the phenomenon of activation by destruction to a Mediator subunit, adding a new mechanism by which Mediator subunits may regulate downstream genes in specific pathways. Furthermore, we show that two novel RING-H2 proteins are involved in the destruction of PFT1, adding new players to this process in plants.

A long-standing question in biology is how the transcription factors, once bound to regulatory elements, communicate with the promoter-bound general transcription factors and the RNA Polymerase II (Pol II) to promote transcription. In eukaryotes, a large complex of about 1 megadalton, called Mediator, plays an essential role in communicating transcription factor activity to the RNA Pol II. The Mediator complex activates transcription and RNA Pol II phosphorylation in vitro. It acts directly on the RNA Pol II and can be purified as a holoenzyme with it (Taatjes, 2010).

Mediator complexes were purified from several eukaryotes (Borggrefe and Yue, 2011), and comparison of genome sequences suggests the conservation of most Mediator subunits across entire kingdoms as well as conservation of the four Mediator subcomplexes: tail, middle, head, and the cyclin-dependent kinase (CDK) modules (Bourbon, 2008).

The plant Mediator complex has been purified (Bäckström et al., 2007). The primary structure of the subunits is not well conserved, but almost all plant Mediator subunits can be identified for their similarity to yeast (*Saccharomyces cerevisiae*) and mammalian Mediator complexes (Bourbon, 2008; Mathur et al., 2011), and secondary structure prediction suggests that overall organization of the complex is also conserved, with the plant Mediator being closer to human Mediator rather than the yeast Mediator (Mathur et al., 2011). Only a few plant Mediator subunits have been functionally characterized. MEDIATOR12 (MED12) and MED13, which are part of the CDK module, are required for proper embryo patterning and also affect flowering time and fertility (Gillmor et al., 2010; Ito et al., 2011; Imura et al., 2012), whereas HUA ENHANCER3, the plant counterpart of CDK8, affects

[1] This work was supported by the Agencia Nacional de Promoción Científica y Tecnológica (grant no. PICT–2006–01593 to P.D.C.), the International Centre for Genetic Engineering and Biotechnology (grant no. CRP/ARG05–02 to P.D.C.), the University of Buenos Aires (grant no. X310 to P.D.C.), and the National Institutes of Health (grant no. 5R01GM52413 to J.C.).

[2] Present address: Instituto de Ciencia y Tecnología Dr. César Milstein, Saladillo 2468, 1440 Buenos Aires, Argentina.

* Corresponding author; e-mail pcerdan@leloir.org.ar.

The author responsible for distribution of materials integral to the findings presented in this article in accordance with the policy described in the Instructions for Authors (www.plantphysiol.org) is: Pablo D. Cerdán (pcerdan@leloir.org.ar).

[W] The online version of this article contains Web-only data.
www.plantphysiol.org/cgi/doi/10.1104/pp.112.205500

floral patterning (Wang and Chen, 2004). The head module components MED17, MED18, and MED20A regulate shoot apical meristem activity, and their absence produces developmental defects (Kim et al., 2011). The tail module component MED14/STRUWWELPETER is also necessary for normal meristem activity, and the corresponding mutants are dwarf and sterile (Autran et al., 2002). Mutations in other subunits produce less evident developmental defects but affect responsiveness to environmental variables: MED16/SENSITIVE TO FREEZING6 regulates freezing tolerance (Knight et al., 2008), and MED25/PHYTOCHROME AND FLOWERING TIME1 (PFT1) and MED8 regulate disease resistance and flowering time (Cerdán and Chory, 2003; Lalanne et al., 2004; Kidd et al., 2009; Iñigo et al., 2012). In turn, other subunits, like MED21, are not viable (Dhawan et al., 2009; Bryant et al., 2011), but viable RNA interference lines also show altered response to pathogens (Dhawan et al., 2009).

The structure of Mediator itself is highly plastic. It was recently proposed that binding of transcription factors to Mediator alters the distribution of Mediator conformations and, hence, affects either the formation of the transcriptional preinitiation complex or the elongation of stalled initiation complexes (Tsai and Nussinov, 2011). Adding to this plasticity, each subunit has the potential to interact with different transcription factors and affect specific pathways (for review, see Borggrefe and Yue, 2011).

The MED25 subunit of both mammals and plants is a good example of how a single subunit can regulate specific responses, at least in part, by interacting with several distinct transcription factors. The mammalian MED25 interacts with several viral transcriptional activators to regulate viral replication (Yang et al., 2004, 2008; Roupelieva et al., 2010; Milbradt et al., 2011; Vojnic et al., 2011), with SOX9 to regulate chondrogenesis (Nakamura et al., 2011), and with the hepatocyte nuclear factor 4α to regulate a specific set of target genes (Rana et al., 2011). The plant MED25/PFT1 binds to at least 19 different transcription factors that include members of at least six different families (Elfving et al., 2011; Ou et al., 2011; Cevik et al., 2012; Chen et al., 2012), and these interactions might be important in regulating a diverse set of processes such as flowering (Cerdán and Chory, 2003; Wollenberg et al., 2008; Iñigo et al., 2012), organ size determination (Xu and Li, 2011), responses to drought (Elfving et al., 2011), jasmonic acid-dependent defense (Kidd et al., 2009; Chen et al., 2012), abscisic acid-induced gene expression (Chen et al., 2012), and light signaling (Cerdán and Chory, 2003; Klose et al., 2012).

The ubiquitin-proteasome system (UPS) plays important roles in the control of transcription using both proteolytic and nonproteolytic capabilities; several proteins, especially in yeast, were found to link transcription with the UPS (Geng and Tansey, 2012). The UPS controls the turnover of transcription factors, and increasing the UPS activity toward a specific transcription factor should decrease the transcription factor activity. However, under several circumstances, it has been shown that, counterintuitively, the proteolysis of acidic transcription factors by the UPS promotes their activity, a phenomenon that was called "activation by destruction" (Lipford et al., 2005). It has been proposed that proteolysis of a spent transcription factor plays a positive role by allowing pristine transcriptional activators to access the promoter to stimulate new rounds of transcription (Geng et al., 2012). These findings were recently extended to nonclassical activators (Wang et al., 2010). Three (and only three) subunits of the yeast Mediator complex (Gal11, Med2, and Pgd1) were able to activate the expression of a β-galactosidase reporter gene when fused to a LexA DNA-binding domain. The three Med-LexA fusions were unstable, and it was shown that at least for Med2-LexA, stabilization of the protein led to decreased activity (Wang et al., 2010).

In this work, we show that PFT1 (the MED25 subunit of the plant Mediator complex, which does not have a counterpart in yeast) is an unstable protein, targeted for degradation by the proteasome, and that this instability is required to activate its target, *FLOWERING LOCUS T* (*FT*), a potent promoter of flowering. Furthermore, we identify two putative E3 ubiquitin ligases that bind to PFT1 in vitro and in yeast and target PFT1 for degradation in vivo. Finally, we show that hypomorphic alleles of these putative E3 ubiquitin ligases delay flowering.

RESULTS

PFT1 Is Degraded by the Proteasome

PFT1 induces flowering time by acting downstream of phytochromes, a group of plant red and far-red light photoreceptors, which are important to monitor the presence of other plants that compete for the light resource (Cerdán and Chory, 2003; Wollenberg et al., 2008). At the molecular level, PFT1 promotes the expression of *FT* (Iñigo et al., 2012), the long-sought plant florigen, which is well known as a flowering integrator gene, because it responds to several pathways that promote flowering (Wigge, 2011). To better understand PFT1 at the biochemical level, we generated epitope-tagged versions of PFT1. We used the PFT1 genomic clone (8,758 bp long) as a whole, without separating coding and noncoding regions. The promoter (2.5 kb) plus the 5′ untranslated region was 2,794 bp long, and the 3′ region was 936 bp long, including about 600 bp after the polyadenylation site. To introduce a minimum of changes in the genomic context, we introduced an *Eco*RI site just before the TAA stop codon to introduce the different tags. We generated transgenic lines bearing *PFT1:TAP* and *PFT1:HA* gene fusions, which complemented the *pft1* late-flowering phenotype (Fig. 1A), indicating that PFT1-tagged versions are functional in vivo. We used a similar approach to generate N-terminal tagged versions, but these constructs did not complement the *pft1* mutant phenotype and were not used for further experiments.

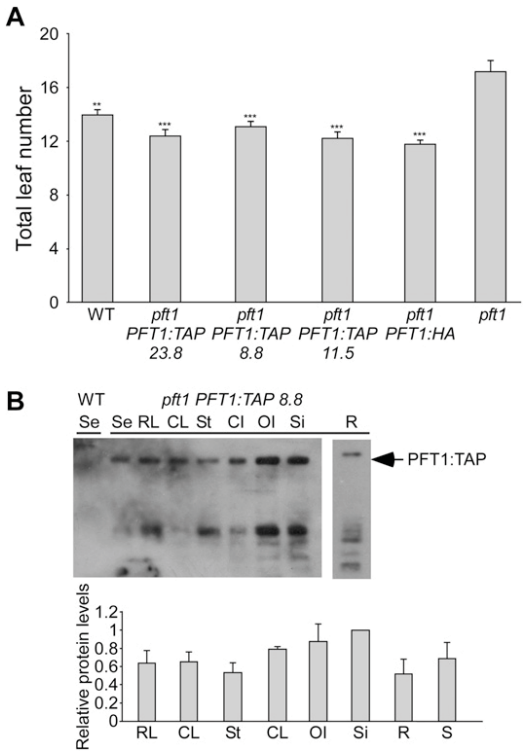

Figure 1. PFT1 protein is unstable and ubiquitously expressed in plants. A, PFT1:TAP and PFT1:HA are functional in vivo. Wild-type plants (WT), *pft1* mutants, and transgenic *pft1* plants complemented with either the *PFT1:TAP* or *PFT1:HA* construct were grown under long days at 23˚C. The total leaf number (cauline and rosette leaves) was recorded at the time of flowering. Independent transgenic lines are indicated by the numbers below each genotype. Bars represent means ± SE of at least 15 plants for each genotype. Asterisks denote statistical significance when comparing *pft1* with complemented lines (**$P < 0.002$, ***$P < 0.001$ by one-way ANOVA and Bonferroni posttests). B, Protein extracts (40 μg per well) of *pft1 PFT1:TAP* lines or wild-type control plants were analyzed by immunoblot. Tissues were obtained from 10-d-old seedlings grown under long days at 23˚C (Se, seedlings; R, roots obtained from seedlings) or from 5-week-old plants (RL, rosette leaf; CL, cauline leaf; St, stem; CI, closed inflorescence; OI, opened inflorescence; Si, siliques). The bottom panel shows the quantification of the PFT1:TAP band (110 kD) relative to PFT1:TAP levels in the silique. Bars represent means ± SE of four independent biological replicates for each tissue.

PFT1 was widely expressed, with somewhat higher levels in reproductive tissue (Fig. 1B). However, degradation products of PFT1:TAP were consistently observed, even if extracts were immediately processed after grinding plant material with liquid nitrogen (Fig. 1B). PFT1 was rapidly degraded in whole plant extracts, with a half-life shorter than 30 min, even in the presence of protease inhibitors (Supplemental Fig. S1). Hence, we tested whether PFT1 was degraded via proteasome. The activity of the proteasome requires ATP and is inhibited by MG132 (Myung et al., 2001). Addition of ATP promoted PFT1 degradation, and most of full-length PFT1 disappeared within 2 min, whereas in control untreated extracts, the full-length PFT1 band was still well detected after 1 h of incubation (Fig. 2A). Addition of MG132 protected PFT1 from degradation, and a strong band corresponding to full-length PFT1 could be observed after 2 h of incubation (Fig. 2A). Addition of MG132 in the presence of ATP extended PFT1 half-life for several minutes, and a faint band could be detected even after 1 h of incubation (Fig. 2A). Then, we tested the effect of MG132 in seedlings and found that MG132 inhibits PFT1 degradation in vivo (Fig. 2, B and C). These results suggest that PFT1 is a target of the proteasome system, although they do not show a regulatory role for this rapid turnover.

PFT1 Degradation Is Intrinsic to Its Regulatory Role

We have previously reported that PFT1:GR-inducible versions of PFT1, in their natural genomic environment, have a strong flowering promotion activity upon the addition of dexamethasone (DXM) when compared with complemented lines (Iñigo et al., 2012). Hence, we

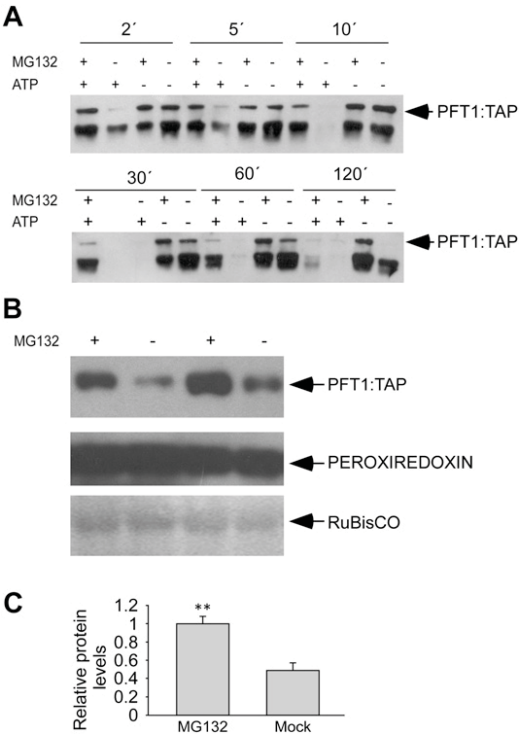

Figure 2. PFT1 is degraded by the proteasome. A, Extracts from 8-d-old seedlings (harvested at 4 h after lights on) were incubated for the times indicated above with 50 μM MG132 or 1% (v/v) DMSO as a mock control with or without 10 mM ATP. Equal amounts of each fraction were then analyzed by immunoblot. B, Ten-day-old seedlings from two independent transgenic lines treated with 100 μM MG132 or 2% (v/v) DMSO as a mock control, harvested 4 h later and processed for immunoblotting. Fifty micrograms of total protein was loaded per well onto an 8% SDS-PAGE gel. Peroxiredoxin and Ponceau-stained Rubisco were used as loading controls. The experiment was repeated with similar results. C, Quantification of PFT1:TAP in independent experiments. Bars represent means ± SE of five independent biological replicates for each treatment.

decided to compare the flowering phenotype and PFT1 protein levels of *PFT1:HA* and *PFT1:GR-HA* lines. Strikingly, PFT1 protein levels were much higher in *PFT1:HA* lines compared with *PFT1:GR-HA* lines, and these differences were not observed at the mRNA level (Fig. 3A; Supplemental Fig. S2). We obtained similar results with two different sources of antibodies (polyclonal and monoclonal), so it is unlikely that the differences were due to changes in the presentation of hemagglutinin (HA) epitopes when fused to the glucocorticoid receptor (GR) domain (Supplemental Fig. S2A). These differences in PFT1 protein levels in *PFT1:HA* and *PFT1:GR-HA* lines did not correlate with flowering time; the strongest effects in the promotion of flowering were found in those lines expressing the lowest levels of PFT1:GR-HA (Fig. 3, A and B).

We reasoned then that PFT1 instability could be important to promote flowering. Hence, we tested the effects of inhibiting the proteasome function in the PFT1-mediated activation of *FT* expression by using the inducible PFT1:GR system (Iñigo et al., 2012). Plants bearing the PFT1:GR fusions rapidly induced the expression of *FT* mRNA in response to DXM (Iñigo et al., 2012; Fig. 3C). However, simultaneous addition of DXM and MG132 abolished the PFT1-mediated activation of *FT* (Fig. 3C). These results strongly suggest that the proteasome-mediated degradation of PFT1 is required for its function in promoting *FT* transcription in a similar manner to that proposed for Gal4 and Med2 in yeast (Lipford et al., 2005; Wang et al., 2010).

PFT1 is involved in other pathways in response to biotic and abiotic stresses (Kidd et al., 2009; Elfving et al., 2011). Hence, we investigated if the proteasome-dependent induction was observed for other PFT1 targets. We tested two pathogen response genes, putative targets of PFT1, *PATHOGENESIS-RELATED4/HEVEIN-LIKE PROTEIN* (*PR4/HEL*) and *PLANT DEFENSIN1.2A* (*PDF1.2A*; Kidd et al., 2009; Ou et al., 2011; Iñigo et al., 2012). *PR4* behaved in a very similar manner to *FT*, but *PDF1.2A* did not (Supplemental Fig. S3). These results suggest that not all PFT1 targets behave in a similar manner and raise the possibility that different signaling cascades and transcription factors acting on PFT1 may have different requirements for PFT1 turnover.

PFT1 Interacts with Two RING-H2 Proteins

The Arabidopsis (*Arabidopsis thaliana*) genome encodes more than 1,000 putative E3 ubiquitin ligases, so it would be very difficult to directly screen for E3 ubiquitin ligases that target PFT1 for degradation in an analogous manner to screenings done in yeast (Lipford et al., 2005; Muratani et al., 2005; Wang et al., 2010). Hence, we conducted a two-hybrid screen in yeast using the von Willebrand factor type A domain of PFT1 (amino acids 1–242) as a bait, a domain that may be involved in protein-protein interactions (Cerdán and Chory, 2003). Six independent clones were isolated, which encode deletion products of two highly similar genes of unknown function, At2g15530 and

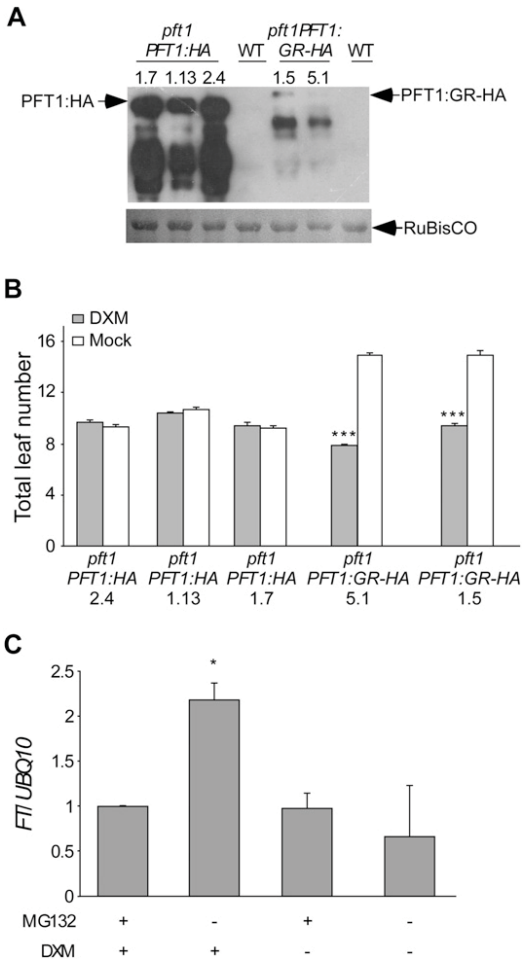

Figure 3. The proteasome-mediated degradation of PFT1 is coupled to its function. A, Plants of the indicated genotypes were grown for 10 d under continuous light at 23°C in MS salts medium supplemented with DXM. After harvesting and grinding, 50 μg of total protein was loaded per well onto an 8% SDS-PAGE gel, and the expression of PFT1:HA and PFT1:GR-HA proteins was examined by immunoblot using monoclonal anti-HA conjugated to peroxidase. Three independent transgenic lines bearing *pft1 PFT1:HA* and two independent transgenic lines bearing *pft1 PFT1:GR-HA* were used. Ponceau staining of the Rubisco protein (bottom panel) is shown as a loading control. WT, Wild type. B, Plants of the indicated genotypes were grown as above in medium supplemented with DXM or ethanol as a control (Mock). The total leaf number (cauline and rosette leaves) was recorded at the time of flowering. Bars represent means ± SE of at least nine plants for each genotype. Asterisks denote the statistical significance of the DXM effect in *pft1 PFT1:GR-HA* and *pft1 PFT1:HA* lines by a Student's *t* test. C, Seedlings (*pft1 PFT1:GR* lines) were grown for 8 d under continuous light and treated for 1 h with 100 μM MG132 or 2% (v/v) DMSO as a mock control and then treated with 1 μM DXM or 0.0096% ethanol as a control for another 3 h before harvesting. Total RNA was extracted, and quantitative reverse transcription-PCR was performed as described in "Materials and Methods" to quantitate *FT* mRNA expression relative to *UBQ10* mRNA after MG132 and DXM treatments. Bars represent means ± SE of two independent experiments with three biological replicates each, each replicate analyzed in triplicate. The asterisk denotes statistical significance when comparing plants treated with DXM and DXM plus MG132 ($P = 0.025$ by a Student's *t* test).

At4g34040 (Fig. 4, A and B; Supplemental Fig. S4A). We named these genes *MED25-BINDING RING-H2 PROTEIN1* (*MBR1*) and *MBR2*, respectively. *MBR1* and *MBR2* encode predicted proteins of 666 and 704 amino acids, respectively, bearing RING-H2 domains close to its C terminus (Fig. 5; Supplemental Fig. S5). The six independent clones spanned different deletions of the N terminus, but the C-terminal halves of both MBR1 (Δ337) and MBR2 (Δ315) were sufficient to interact with PFT1 amino acids 1 to 242, either fused to the GAL4 binding domain or the GAL4 activation domain (Fig. 4, A and B; Supplemental Fig. S4A). However, the RING-H2 domain alone (amino acids 599–704 of MBR1) was not sufficient (Fig. 4A). By contrast, we did not detect significant interactions with another gene product that bears a similar RING-H2 domain (At5g42940, named MBRL2; Figs. 4A and 5). Interestingly, the N-terminal portion of MBR1 was necessary to activate transcription in yeast, suggesting that the C-terminal halves of MBR1 and MBR2 interact with PFT1 whereas the N-terminal halves may have a transcriptional role (Fig. 4, A and B; Supplemental Fig. S4B).

Next, we sought to test the binding of MBRs and PFT1 in vitro. We prepared recombinant MBR2 (Δ315) and MBR1 (Δ337) as fusions to the MALTOSE-BINDING PROTEIN (MBP) of *Escherichia coli*. Only MBP:MBR2 (Δ315) was expressed, whereas MBR1 (Δ337) was not, either as an MBP fusion or as a glutathione *S*-transferase fusion. We used the MBP:MBR2 (Δ315) fusion protein to prepare affinity columns by immobilizing MBP:MBR2Δ315 to amylose resin. When we loaded plant extracts from PFT1:TAP lines, we observed that PFT1 was retained in the column and hardly detected in the flow through. C-terminal fragments of PFT1 were still retained in the column, although washed easily, suggesting that the C-terminal portion of PFT1 may contribute to the interactions with MBR proteins or may be retained by other Mediator-associated proteins. In contrast, no retention was observed with control columns bound to MBP alone (Fig. 4C). The binding of PFT1 may not be strong under these in vitro conditions, because thorough washing removed PFT1, but still a significant portion remained bound to the columns and was eluted with maltose (Fig. 4C). PFT1:HA fusions were also retained by MBR2Δ315 immobilized columns (data not shown), indicating that binding to MBR2 is independent of the tag. We also found that PFT1:TAP was retained in columns when MBP-MBR2 (Δ315) was cross-linked to a *N*-hydroxysuccinimide-activated Sepharose 4 Fast Flow matrix (Supplemental Fig. S4C). These results show that PFT1 not only interacts with MBR2 in the two-hybrid system but also in vitro.

MBR1 and MBR2 Belong to a Small Family of Putative E3 Ubiquitin Ligases

MBR1 and MBR2 are 64.6% identical. Only two other proteins in the Arabidopsis genome, At1g45180 and At5g42940, contain both a similar RING-H2 domain close to the C terminus and a similar set of conserved amino acids in their N-terminal portion (SCKRKAL); we named them MBR-like1 (MBRL1) and MBRL2, respectively (Fig. 5; Supplemental Fig. S5). Hence, this small family comprises four members out of 465 putative Arabidopsis RING-H2 proteins (Santner and Estelle, 2010).

We tested the expression patterns of these four genes. *MBR1* mRNA was quite ubiquitous; we found it in vegetative and reproductive tissue. *MBR2* mRNA was found mostly in vegetative tissue, cauline leaves, rosette leaves, and stem. *MBRL1* mRNA was found in all tissues tested but with lower levels in leaves, whereas

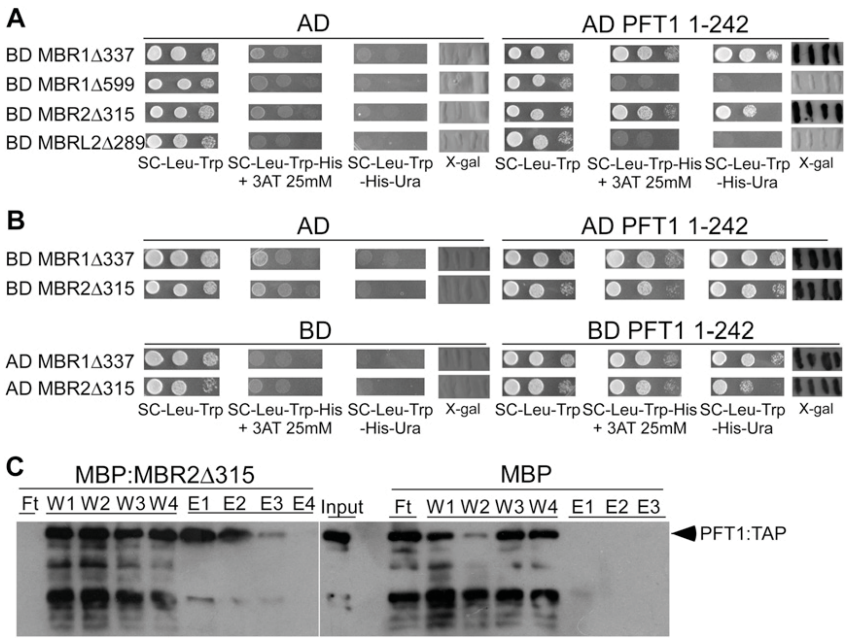

Figure 4. MBR1 and MBR2 interact with PFT1. A and B, Yeast two-hybrid assay between PFT1 amino acids 1 to 242 and N-terminal deletions of either MBR1 or MBR2. Grown cultures were diluted to 10^{-2} and 10^{-3} and then spotted on nonselective SC-Leu-Trp, selective SC-Leu-Trp-His supplemented with 25 mM 3-amino-1,2,4-triazole (3AT), and SC-Leu-Trp-His-Ura media plates. 5-bromo-4-chloro-indolyl-β-D-galactopyranoside (X-gal) was used for the detection of β-Gal activity, according to the ProQuest manual (Invitrogen). AD, GAL4 activation domain; BD, GAL4 DNA-binding domain. C, PFT1 interacts with MBR2Δ315 in vitro. Total proteins were extracted from 10-d-old *pft1 PFT1:TAP* seedlings and loaded onto a 1-mL amylose affinity column containing either MBP:MBR2Δ315- or MBP (control)-bound proteins. W1 to W4 and E1 to E4 correspond to wash and elution fractions (28% of each), respectively. Ft, Flow through. For input, 3% of total protein extract was loaded. The experiment was repeated with similar results.

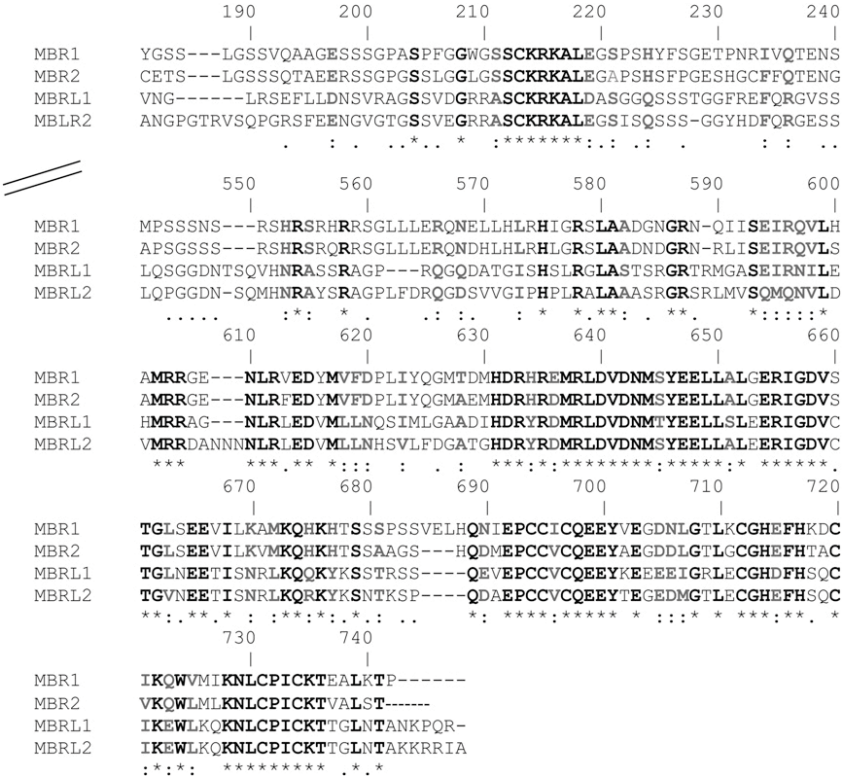

Figure 5. MBR1, MBR2, MBRL1, and MBRL2 show similarity beyond the RING-H2 domain. Sequence alignment, using the ClustalW program, of N-terminal portions (amino acids 180–240), including the conserved set of amino acids SCKRKAL, and sequence alignment of the C-terminal domain containing RING-H2 domains of MBR1, MBR2, MBRL1, and MBRL2 are shown. Asterisks denote conserved residues, and double and single dots indicate semiconserved amino acids.

MBRL2 showed low levels of mRNA in most tissues except for cauline leaves (Supplemental Fig. S6).

Testing ubiquitin ligase activity directly has not been straightforward for these proteins (Stone et al., 2005), but in similar circumstances, binding to ubiquitin conjugases (UBC) has been an important piece of evidence to classify E3 ubiquitin ligases (Peng et al., 2007). The Arabidopsis genome contains 37 UBC genes (Kraft et al., 2005). Large-scale interactome projects have made some advancements in this field, and there is evidence indicating that At5g42940 (MBRL2) interacts with UBC9 and UBC11 (Arabidopsis Interactome Mapping Consortium, 2011). Therefore, we tested the interactions between MBR1 and MBR2 with UBC8, UBC9, and UBC11. We did not find significant interactions with UBC8 and UBC9, but we detected significant interactions between MBR1 and MBR2 with UBC11 (Supplemental Fig. S7). These data, together with the presence of the typical RING-H2 domain, strongly suggest that MBR1 and MBR2 are bona fide ubiquitin ligases.

MBR1 and MBR2 Lower the Levels of PFT1 in a RING-H2 Domain-Dependent Fashion

To test directly the hypothesis that PFT1 is a target of MBR1 and MBR2 in vivo, we performed agroinfiltration experiments to transiently coexpress PFT1:TAP and either MBR1 or MBR2. Coexpression of MBR1 or MBR2 with PFT1:TAP produced a significant decrease in the PFT1:TAP protein levels (Fig. 6A). A similar experiment was performed using PFT1:HA versions instead of PFT1:TAP, with similar results, indicating that the effects are tag independent (Supplemental Fig. S8).

RING-H2 domains are essential for E3 ubiquitin ligase activity (Stone et al., 2005), so we decided to test whether the degradation of PFT1 was dependent on the RING-H2 of MBR2. We mutated the two conserved His amino acids to Ala, because these conserved His residues are known to bind Zn^{2+}. The MBR2AA mutated version did not promote PFT1 degradation, showing that the RING-H2 domain is required for activity (Fig. 6B).

PFT1 Levels Are Increased in *mbr1 mbr2* Double Mutants and *MBR1* and *MBR2* Knockdowns

To further test the role of MBR1 and MBR2 in planta, we searched T-DNA insertion collections for putative *mbr1* and *mbr2* knockouts. We found two insertional alleles for *mbr2*, named *mbr2-1* and *mbr2-2* (lines SAIL_870_B03 and GABI_587C07, respectively; McElver et al., 2001; Rosso et al., 2003). Both T-DNAs were inserted within the second intron, surrounded by coding exons (Supplemental Fig. S9B). The *MBR2* mRNA levels were barely detectable in *mbr2-1* alleles (Supplemental Fig. S9C). By contrast, we only found a single T-DNA line available for *MBR1* (SALK_048290; Alonso et al., 2003) in the Columbia ecotype. This T-DNA was inserted in the fifth intron of the *MBR1* gene (Supplemental Fig. S9A). However, significant levels of *MBR1* mRNA were detected in *mbr1-1* (Supplemental Fig. S9C), and reverse

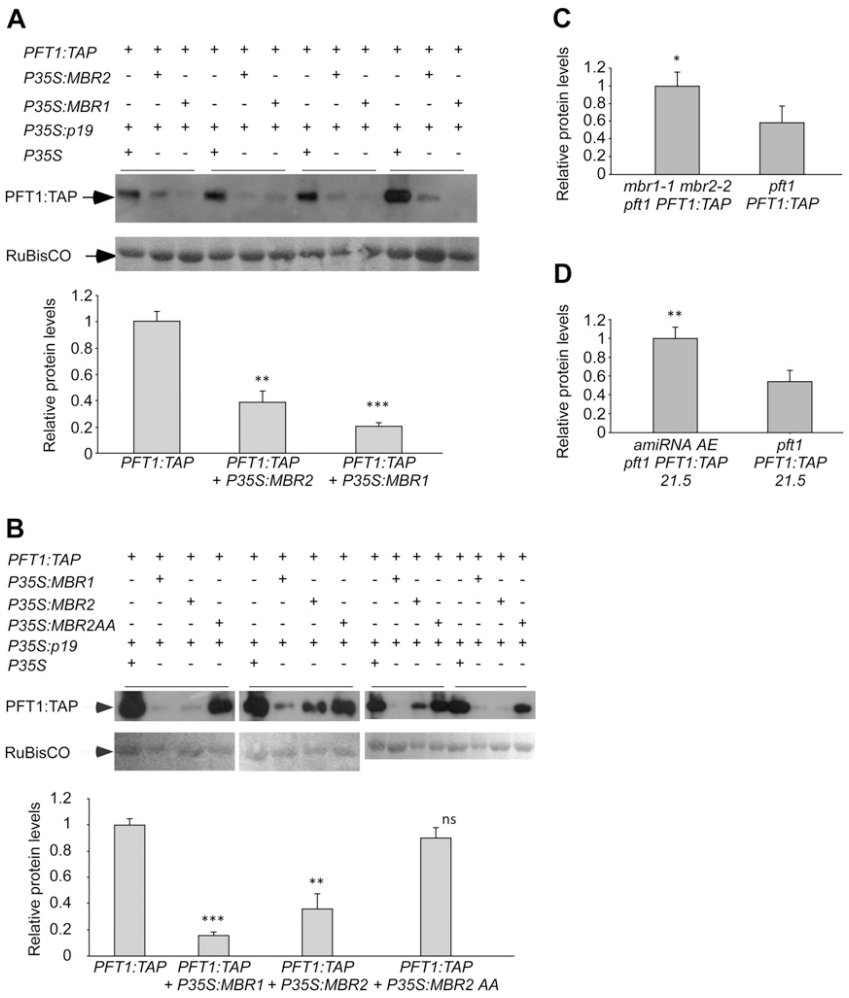

Figure 6. MBR1 and MBR2 promote PFT1 degradation in vivo in a RING-H2 domain-dependent way. A, The indicated constructs were transiently coexpressed in *N. benthamiana* leaves by agroinfiltration, followed by immunoblotting (four independent agroinfiltrations are shown). Ponceau staining of the Rubisco protein is shown as a loading control. The bottom panel shows the quantification of the PFT1:TAP band. Bars represent means ± SE of four independent samples. Asterisks indicate significance levels after a Student's *t* test as follows: $^{**}P < 0.01$, $^{***}P < 0.001$. B, Constructs were transiently coexpressed and analyzed as in A. The MBR2AA construct bears two His-to-Ala mutations that disrupt the zinc-binding domain of the RING-H2 domain. ns, Not significant. C and D, Seedlings of the indicated genotypes were grown for 10 d in long days and processed for immunoblotting to quantify PFT1:TAP. Data represent means ± SE of at least three independent samples for each genotype. $^{*}P < 0.05$.

transcription-PCR followed by sequencing showed that the T-DNA insertion was being spliced out of the *MBR1* mRNA. In spite of *MBR1* mRNA levels being 20% of the wild-type levels in the *mbr1-1* mutant, this mRNA had the wild-type sequence, so it was expected to give a significant amount of MBR1 protein. Hence, we also generated knockdowns for *MBR* genes using artificial microRNAs (amiRNAs; Ossowski et al., 2008). First, we generated two different amiRNAs to target *MBR1* and *MBR2* mRNAs (identified with letters B and V) and two other tandem amiRNAs (identified with letters AE and VC) to target both *MBR1* and *MBR2* and both *MBRL1* and *MBRL2* mRNAs (Supplemental Fig. S9, D and E). Despite the fact that we did not have evidence of MBRL1 or MBRL2 interacting with PFT1, knocking down *MBRL1* and *MBRL2* mRNAs could uncover potential redundancy. We generated *mbr1 mbr2 pft1 PFT1:TAP* lines and knockdown *amiRNA AE pft1 PFT1:TAP* lines. In both cases, low levels of *MBR* mRNA (Supplemental Figs. S9C and S10, B–E) correlated with higher PFT1:TAP protein levels (Fig. 6, C and D), suggesting that MBR proteins promote PFT1 degradation in planta at physiological levels.

Low Levels of MBR1 and MBR2 Produce a Delay in Flowering Onset

Given that PFT1 promotes flowering (Iñigo et al., 2012) and PFT1 proteolysis by the UPS system is required for full PFT1-promoting activity, we reasoned that *MBR* loss-of-function mutants should flower later than the wild type. Single *mbr1-1* and *mbr2-1* mutants did not flower significantly different from wild-type plants (Fig. 7A). However, the *mbr1-1 mbr2-1* double mutants flowered later than wild-type plants, indicating that MBR1 and MBR2 act redundantly in the control of flowering (Fig. 7A). The effect on flowering of the double mutants was statistically significant but subtle, more likely due to the significant expression of *MBR1* in *mbr1-1* mutants (Supplemental Fig. S9C).

We confirmed the late-flowering phenotype of *mbr1 mbr2* double mutants by using the knockdown lines. In an initial assessment, six out of 13 homozygous and single-locus-insertion transgenic lines targeting *MBR1* and *MBR2* flowered later than the wild type (Supplemental Fig. S10A). We selected some lines displaying weak and strong effects and confirmed the late-flowering phenotype, which correlated

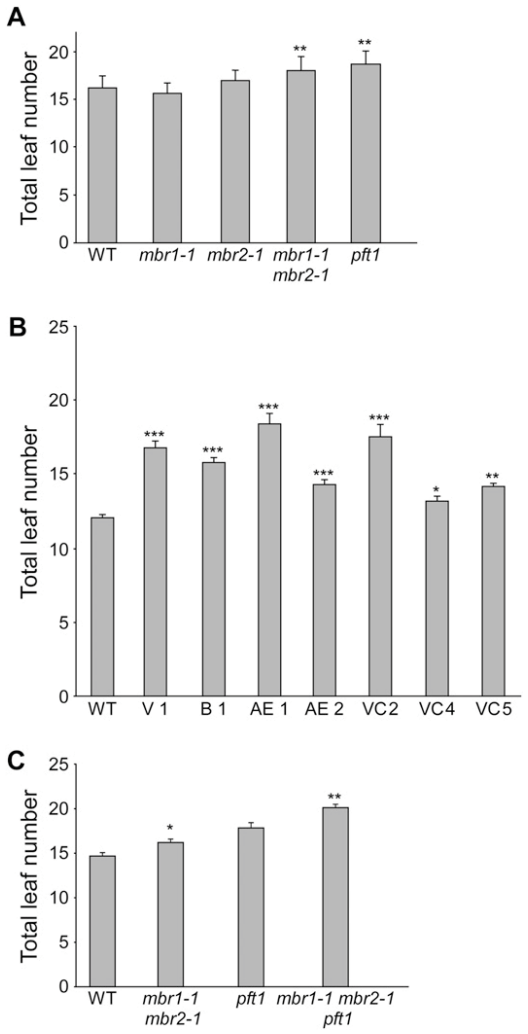

Figure 7. MBR1 and MBR2 promote flowering. A, Plants of the indicated genotypes were grown under long days at 23°C. The total leaf number (cauline and rosette leaves) was recorded at the time of flowering. Bars represent means ± SE of five independent experiments including at least 58 plants for each genotype. Asterisks denote statistical significance when compared with the wild type (WT) by a type II ANOVA for repeated measures, as follows: $^{**}P < 0.01$. B, Flowering time experiment as in A. Data represent means ± SE of at least six plants for each genotype (for another experiment with similar results, see Supplemental Fig. S10A). Asterisks denote statistical significance by a one-way ANOVA and Bonferroni post-tests, as follows: $^{*}P < 0.05$, $^{**}P < 0.01$, $^{***}P < 0.001$. V 1 and B 1 are transgenic lines targeting *MBR1* and *MBR2* with two different amiRNAs; AE and VC are transgenic lines targeting *MBR1*, *MBR2*, *MBRL1*, and *MBRL2* with two different tandem amiRNAs (AE and VC). C, Flowering time experiment as in A. Data represent means ± SE of at least 22 plants for each genotype. The experiment was repeated with similar results. Asterisks denote statistical significance when *mbr1-1 mbr2-1 pft1* lines were compared with *pft1-1* plants and *mbr1-1 mbr2-1* double mutants were compared with wild-type plants by a Student's *t* test, as follows: $^{*}P < 0.05$, $^{**}P < 0.01$.

with *MBR* expression levels in these lines (Fig. 7B; Supplemental Fig. S10, B–E).

The late-flowering phenotype of *mbr1 mbr2* double mutants and *MBR* knockdown lines was consistent with their role in promoting the turnover of PFT1, which is necessary for its function in promoting *FT* expression. However, the strongest knockdown lines also displayed a leaf phenotype not observed in *pft1* mutants, suggesting possible PFT1-independent roles for MBR1 and MBR2 (Supplemental Fig. S10F). Hence, to test whether MBR1 and MBR2 could regulate flowering in a PFT1-independent manner, we measured the flowering time of *mbr1 mbr2* double mutants in the *pft1* mutant background. Once again, the *mbr1 mbr2* double mutants flowered later than wild-type plants (Fig. 7C). However, the triple mutants *mbr1 mbr2 pft1* flowered significantly later than the *mbr1 mbr2* double mutants, indicating that MBR1 and MBR2 also contribute to flowering control by at least one PFT1-independent mechanism (Fig. 7C).

DISCUSSION

The UPS is now recognized as a very important regulator of several steps during gene transcription, and its proteolytic activity is essential in several of the proteasome roles. This is highlighted by the recent finding that the yeast 26S complex of the proteasome associates with transcriptionally active chromatin and dissociates rapidly once transcription is shut down (Geng and Tansey, 2012). Original work by the Tansey laboratory has shown an overlap of activation domains within acidic transcription factors and the elements that signal destruction by the proteasome. That team also found a close correlation between the ability of an acidic activation domain to activate transcription and to signal proteolysis (Salghetti et al., 2000). Further mechanistic insights were obtained from experiments done in yeast; it was shown that the capacity of transcriptional activators VP16 and GCN4 to recruit RNA Pol II, but not their DNA binding capacity, depended on the activity of specific ubiquitin ligases (Salghetti et al., 2001; Lipford et al., 2005). The observation of correlation between the instability and the ability to promote gene expression was extended to nonacidic transcriptional coactivators, including Med2 in yeast (Wang et al., 2010).

In this study, we show that PFT1, the MED25 subunit of the plant Mediator complex, is a highly unstable protein, degraded via proteasome both in vitro and in vivo (Fig. 2). We also show that blocking the activity of the proteasome precludes activation of *FT* by PFT1 (Fig. 3C). Furthermore, we identified a role for two putative E3 ubiquitin ligases, of previously unknown function, as regulators of PFT1 stability. MBR1 and MBR2, the two putative E3 ubiquitin ligases, contain canonical RING domains (of the type C3H2C3) close to the C terminus and were classified in group I, among the 469 predicted Arabidopsis RING domain-containing proteins (Stone et al., 2005). Ubiquitin ligase activity for MBR1 and MBR2 was not observed when using UBC8 as the E2 conjugase (Stone et al., 2005). Our experiments show that MBR1 and MBR2 do not bind to UBC8 in yeast, but they do bind to UBC11, further supporting their role as E3 ubiquitin ligases.

Nevertheless, it is still unclear which of the 37 UBC E2s identified in the Arabidopsis genome would be the partners for MBR1 and MBR2 in planta (Kraft et al., 2005). By homology searches, we found two other similar proteins to MBR1 and MBR2 in the Arabidopsis genome, which we named MBRL1 and MBRL2. These two proteins have similar RING domains and also conserved sequences in the N-terminal portion (Fig. 5; Supplemental Fig. S5), but we did not find evidence to support a role in the regulation of PFT1 protein levels.

We found several pieces of evidence showing that MBR1 and MBR2 promote the degradation of PFT1 in vivo: (1) MBR proteins interacted with PFT1 in yeast and in vitro (Fig. 4; Supplemental Fig. S4); (2) MBR proteins promoted the degradation of PFT1 in planta, in a RING domain-dependent way (Fig. 6; Supplemental Fig. S8); and (3) partial loss of function of MBR proteins led to higher levels of PFT1 (Fig. 6, C and D).

PFT1 is a positive regulator of flowering that acts by promoting the expression of *FT* (Iñigo et al., 2012). The data presented so far suggest that MBR proteins are involved in the degradation of PFT1 by the UPS and that this degradation is important to induce the expression of *FT* and, consequently, to promote flowering. Consistent with this proposition, we found that *mbr1 mbr2* double mutants flowered later than the wild type, and these results were confirmed with knockdown lines (Fig. 7, A and B; Supplemental Fig. S10). Different amiRNAs targeting both *MBR1* and *MBR2* or *MBR* and *MBRL* genes gave similar results, indicating that the effects were specific and not the product of knocking down off-targets.

Nevertheless, some knockdown lines displayed a leaf phenotype that we did not observe in *pft1* mutants (Supplemental Fig. S10F), and our genetic analysis indicated that MBRs were also able to regulate flowering independently of PFT1 (Fig. 7C). At present, it is unclear which other targets for MBR1 and MBR2 are present within the Arabidopsis genome. However, other Mediator subunits, like MED8, can promote flowering independently of PFT1 (Kidd et al., 2009) and could be direct or indirect targets of MBR proteins to regulate flowering by a PFT1-independent mode.

In contrast to PFT1, neither MBR1 nor MBR2 was reported as part of the Mediator complex (Bäckström et al., 2007), thus suggesting that the interaction may be transient in vivo or that these proteins bind to the free PFT1 form, not found in the context of Mediator. In gel filtration experiments, we found that more that 50% of PFT1 was associated with high-M_r complexes consistent with Mediator size (data not shown). The results of affinity chromatography showing that most of PFT1 was retained in the columns with immobilized MBR2 (Fig. 4C) suggest that MBR proteins are able to bind PFT1 in the context of Mediator. However, we cannot exclude that MBR proteins exert their role by binding to free PFT1 and that this free form has an important role in transcription. In mammalian systems, substantial amounts of MED25 were found in an unbound state, and this free form was indeed found to be involved in transcription and to recruit Mediator to promoters. Kinetics analysis showed that MED25 associated first with promoters and then recruited other Mediator subunits (Lee et al., 2007). In a very recent paper, these findings were extended to Arabidopsis PFT1 (Chen et al., 2012). Our results on PFT1 are also reminiscent of observations in yeast. When yeast Med2 is fused to a DNA-binding domain, it turns into an unstable protein and seems to recruit Mediator to promoters, activating transcription (Wang et al., 2010).

The fact that some of the targets of PFT1, which are part of the pathogen response pathway, did not respond to the blockage of PFT1 degradation (*PR4* behaved in a very similar manner to *FT*, but *PDF1.2A* did not; Supplemental Fig. S3) raises the possibility that different signaling cascades and transcription factors acting on PFT1 may have different requirements for PFT1 turnover. The N-terminal domain of PFT1, which binds to MBR proteins, is conserved in human Mediator, but this domain is different from the ACID domain, which interacts with at least 19 different transcription factors (Elfving et al., 2011; Ou et al., 2011; Cevik et al., 2012; Chen et al., 2012). Hence, PFT1 could potentially integrate different signaling pathways by binding to very different transcription factors and at the same time bind to MBR proteins. The results of these tripartite interactions could be different, depending on the transcription factor involved. Hence, our results raise the possibility that binding of MBR proteins and interaction with the UPS could potentially result in another regulatory layer to ensure that PFT1 delivers the correct output to the transcription machinery.

The UPS-mediated proteolysis of transcription factors and coactivators was also shown to affect gene expression by posttranscriptional mechanisms, rendering mRNAs untranslatable, possibly by uncoupling processes that initiate transcription with processes that elongate transcripts (Muratani et al., 2005). A similar situation was also shown for yeast Med2, although the mechanistic details are largely unknown (Wang et al., 2010). Whether PFT1 also affects the fate of mRNAs after transcription is currently unknown and will require thorough investigations.

The UPS-mediated activation of transcription factor activity might be a more extended process in Arabidopsis than previously anticipated. For example, during flower development, UNUSUAL FLORAL ORGANS, an F-box protein that forms an SCF ubiquitin ligase, acts together with the transcription factor LEAFY (LFY) to induce the transcription of LFY downstream targets in a proteasome-dependent way (Chae et al., 2008).

In vertebrate systems, the MED25 subunit interacts with Wwp2, a HECT domain E3 ubiquitin ligase (Rotin and Kumar, 2009). This interaction is required to form a complex with Sox9, which is required for downstream gene expression and palatogenesis. However, by contrast to our results in plants, Wwp2 did not stimulate the degradation of either Med25 or Sox9 (Nakamura et al., 2011). It would be interesting to know if other

contexts, or other ubiquitin ligases, may promote Med25 turnover in vertebrate systems, as we found in Arabidopsis. Another mammalian Mediator subunit, Med8, also interacts with E3 ubiquitin ligases, which contain the RING protein Rbx1. The E3 ubiquitin ligase activity is recruited to the Mediator complex, but it is still unclear if any of the Mediator subunits are substrates for this activity (Brower et al., 2002).

Our results further advance the understanding of the functional importance of the interactions between the Mediator complex subunits and the proteasome pathway by presenting evidence that PFT1, the plant MED25 subunit, binds to E3 ubiquitin ligases, which promotes its degradation, and that the degradation of PFT1 is functionally important to promote the transcription of downstream target genes.

MATERIALS AND METHODS

Plant Material

All the alleles and transgenic lines used were in the Arabidopsis (*Arabidopsis thaliana*) Columbia background: *pft1-1* (Cerdán and Chory, 2003), *mbr1-1* (At2g15530; SALK_048290), *mbr2-1* (At4g34040; SAIL _870_B03), and *mbr2-2* (At4g34040; GABI_587C07; McElver et al., 2001; Alonso et al., 2003; Rosso et al., 2003).

Plant Growth Conditions

Plants were grown on a 1:1:1 soil:vermiculite:perlite mixture at 23°C under long days (16 h of light/8 h of dark) or continuous light, with a light intensity of 80 μmol m^{-2} s^{-1} produced by cool-white fluorescent tubes, and fertilized every 2 weeks with a 0.1% solution of Hakaphos (Compo Agricultura).

Murashige and Skoog (MS) salts were used for in vitro culture, and where indicated, the medium was supplemented with 1 μM DXM (Sigma; D1756) or 0.0096% ethanol as a mock control.

Constructs

For PFT1 constructs, an *Eco*RI site was engineered just before the TAA stop codon of the complete genomic clone. The tags were subcloned in this *Eco*RI site within the binary plasmid pPZP212. These constructs were used to transform plants with *Agrobacterium tumefaciens* GV3101 (Clough and Bent, 1998). Only lines showing a 3:1 segregation ratio in the T2, indicating single-locus insertions, were used for subsequent experiments.

P35S:MBR1 and *P35S:MBR2* fusion constructs were created by cloning the respective cDNAs into the CHF3 binary vector. In the *P35S:MBR2AA* fusion, the amino acids 639 and 642 were mutated to Ala by site-directed mutagenesis.

MBR2Δ315 was expressed from pMAL-c2 vector (New England Biolabs).

The amiRNA constructs directed against *MBR1* and *MBR2* genes were designed using WMD2 Web Micro RNA designer (http://wmd2.weigelworld.org/cgi-bin/mirnatools.pl; Ossowski et al., 2008). Overlapping PCR was used to replace MIR319a precursor by each amiRNA and finally subcloned into CHF3 or CHF1 binary vectors for plant transformation. Transgenic lines were selected on MS medium supplemented with 50 μg mL^{-1} kanamycin or 100 μg mL^{-1} gentamycin.

Yeast Strains and Yeast Two-Hybrid Screening

Yeast (*Saccharomyces cerevisiae*) strain MAV203 and pBDLeu and pEXPAD vectors were used for yeast two-hybrid assays (ProQuest System; Invitrogen). The cDNA library was constructed from total RNA isolated from Arabidopsis inflorescences (Wigge et al., 2005) and was a generous gift from Philip Wigge and Detlef Weigel. The yeast complete medium (yeast extract peptone dextrose adenine) and the different synthetic dropout (synthetic complete [SC]) media were purchased from Difco and Clontech, respectively, and prepared as suggested by the manufacturers.

Agroinfiltration Procedure

For coinfiltration, equal volumes of different *A. tumefaciens* strains (GV3101) carrying different constructs were first mixed and then applied to the abaxial side of 4- to 6-week-old *Nicotiana benthamiana* leaves by using a 1-mL syringe (without needle). In all cases, leaves were coinfiltrated with binary plasmid pBIN61-p19 bearing the p19 silencing suppressor under the control of the P35S promoter (Voinnet et al., 2003). Three days after agroinfiltration, leaves were harvested and frozen in liquid N_2 for further processing.

Quantitative Reverse Transcription-PCR

Total RNA extraction, cDNA synthesis, and quantitative PCR with SYBR Green I (Invitrogen) were performed essentially as described previously (Iñigo et al., 2012). For primers and full details, see Supplemental Materials and Methods S1.

Protein Extraction and Immunoblots

Protein extracts were prepared by resuspending ground tissue in cold extraction buffer (50 mM Tris-HCl, pH 7.5, 150 mM NaCl, 0.1% [p/v] Nonidet P-40, and 10% glycerol) at a ratio of 1 g tissue mL^{-1} extraction buffer and then centrifuged at 13,000*g* for 30 min. When necessary, aliquots were stored at −80°C to quantify proteins by the method of Lowry et al. (1951). When used for gel loading, 1 volume of 2× SDS sample buffer was added to each extract and boiled for 5 min. Unless otherwise stated, 40 μg of protein per sample was subjected to 8% to 10% SDS-PAGE and transferred to a nitrocellulose membrane (Hybond-ECL; Amersham Biosciences; RPN303D).

Antibodies used were as follows: TAP, peroxidase anti-peroxidase soluble complex antibody (Sigma P1291); HA, anti-HA peroxidase (Roche 3F10; 2013819) or polyclonal anti-HA (Sigma H6908) followed by anti-rabbit IgG peroxidase (Sigma A0545). The signal was developed with the Millipore chemiluminescent horseradish peroxidase substrate kit. Bands were quantified by using ImageJ software.

PFT1 Stability Assays

MG132 (Sigma C2211) was used at a final concentration of 50 μM, 1% (v/v) dimethyl sulfoxide (DMSO) as a control, and 10 mM ATP (final). Each reaction was incubated at room temperature, and samples were removed at different time points. The reaction was stopped by the addition of SDS sample buffer and boiling for 5 min before gel analysis.

The stability of PFT1 in the presence of protease inhibitors was tested as above, but using a protease inhibitor cocktail (Sigma P9599) at a concentration of 3% (v/v).

To test the role of the proteasome in vivo, *pft1 PFT1:TAP* seedlings were grown under long days at 23°C in MS medium supplemented with 1% (p/v) Suc for 10 d. During day 10, 2 h after dawn, seedlings were covered with 100 μM MG132 or 2% (v/v) DMSO. Samples were harvested 4 h later and subjected to immunoblot analysis.

Expression of MBP:MBR2Δ315 Fusion Protein, and Affinity Column-Binding Assays

The *MBP:MBR2Δ315* fusion was expressed in *Escherichia coli* strain BL21-pLysS. Protein purification was carried out with amylose resin (New England Biolabs E8021) according to the manufacturer's instructions. For affinity chromatography, MBP:MBR2Δ315 or MBP alone was loaded onto a 1-mL Amylose Resin High Flow (New England Biolabs E8022S) or coupled to *N*-hydroxysuccinimide-activated Sepharose 4 Fast Flow (GE 17-0906-01). These resins were used for protein-binding assays using plant extracts prepared from 500 mg of tissue (for details, see Supplemental Materials and Methods S1).

Sequence data from this article can be found in The Arabidopsis Information Resource and in the GenBank/EMBL data libraries under the following accession numbers: *PFT1* (At1g25540), *MBR1* (At2g15530), *MBR2* (At4g34040), *MBRL1* (At1g45180), *MBRL2* (At5g42940), *FT* (At1g65480), *PR4* (At3g04720), *PDF1.2A* (At5g44420), *UBQ10* (At4g05320), *UBC8* (At5g41700), *UBC9* (At4g27960), and *UBC11* (At3g08890).

Supplemental Data

The following materials are available in the online version of this article.

Supplemental Figure S1. Protease inhibitors do not protect PFT1:TAP from degradation.

Supplemental Figure S2. PFT1:HA and PFT1:GR-HA protein levels show an inverted correlation with their capacity to promote flowering.

Supplemental Figure S3. Blockage of PFT1 destruction impairs the induction of *PR4* but not *PDF1.2*.

Supplemental Figure S4. Binding of PFT1 in yeast and in vitro.

Supplemental Figure S5. Complete sequence alignment of MBR1, MBR2, MBRL1, and MBRL2.

Supplemental Figure S6. Expression of *MBR1*, *MBR2*, *MBRL1*, and *MBRL2* in different plant organs.

Supplemental Figure S7. MBR1 and MBR2 interact with UBC11 in yeast.

Supplemental Figure S8. MBR1 and MBR2 promote PFT1 degradation in vivo.

Supplemental Figure S9. Isolation of *MBR1* and *MBR2* mutants and knockdowns.

Supplemental Figure S10. Phenotypes of *MBR1* and *MBR2* suppressor lines.

Supplemental Materials and Methods S1.

ACKNOWLEDGMENTS

We are grateful to the Arabidopsis Biological Resource Center Stock Center for seed stocks, Detlef Weigel and Philip Wigge for the cDNA library, Eliott Meyerowitz and Frank Wellmer for the original GR construct, Christian Fankhauser for the CHF5 vector, David Baulcombe for the P35S:p19 construct in pBin61, Ricardo Wolosiuk for peroxiredoxin antiserum, Judy Callis for UBC8 cDNA and useful suggestions, and Jorge Casal, Marcelo Yanovsky, and Santiago Mora-García for useful comments on the manuscript.

Received August 13, 2012; accepted September 17, 2012; published September 19, 2012.

LITERATURE CITED

Alonso JM, Stepanova AN, Leisse TJ, Kim CJ, Chen H, Shinn P, Stevenson DK, Zimmerman J, Barajas P, Cheuk R, et al (2003) Genome-wide insertional mutagenesis of Arabidopsis thaliana. Science **301:** 653–657

Arabidopsis Interactome Mapping Consortium (2011) Evidence for network evolution in an Arabidopsis interactome map. Science **333:** 601–607

Autran D, Jonak C, Belcram K, Beemster GT, Kronenberger J, Grandjean O, Inzé D, Traas J (2002) Cell numbers and leaf development in Arabidopsis: a functional analysis of the STRUWWELPETER gene. EMBO J **21:** 6036–6049

Bäckström S, Elfving N, Nilsson R, Wingsle G, Björklund S (2007) Purification of a plant mediator from Arabidopsis thaliana identifies PFT1 as the Med25 subunit. Mol Cell **26:** 717–729

Borggrefe T, Yue X (2011) Interactions between subunits of the Mediator complex with gene-specific transcription factors. Semin Cell Dev Biol **22:** 759–768

Bourbon HM (2008) Comparative genomics supports a deep evolutionary origin for the large, four-module transcriptional mediator complex. Nucleic Acids Res **36:** 3993–4008

Brower CS, Sato S, Tomomori-Sato C, Kamura T, Pause A, Stearman R, Klausner RD, Malik S, Lane WS, Sorokina I, et al (2002) Mammalian mediator subunit mMED8 is an Elongin BC-interacting protein that can assemble with Cul2 and Rbx1 to reconstitute a ubiquitin ligase. Proc Natl Acad Sci USA **99:** 10353–10358

Bryant N, Lloyd J, Sweeney C, Myouga F, Meinke D (2011) Identification of nuclear genes encoding chloroplast-localized proteins required for embryo development in Arabidopsis. Plant Physiol **155:** 1678–1689

Cerdán PD, Chory J (2003) Regulation of flowering time by light quality. Nature **423:** 881–885

Cevik V, Kidd BN, Zhang P, Hill C, Kiddle S, Denby KJ, Holub EB, Cahill DM, Manners JM, Schenk PM, et al (2012) MEDIATOR25 acts as an integrative hub for the regulation of jasmonate-responsive gene expression in Arabidopsis. Plant Physiol **160:** 541–555)

Chae E, Tan QK, Hill TA, Irish VF (2008) An Arabidopsis F-box protein acts as a transcriptional co-factor to regulate floral development. Development **135:** 1235–1245

Chen R, Jiang H, Li L, Zhai Q, Qi L, Zhou W, Liu X, Li H, Zheng W, Sun J, et al (2012) The *Arabidopsis* Mediator subunit MED25 differentially regulates jasmonate and abscisic acid signaling through interacting with the MYC2 and ABI5 transcription factors. Plant Cell **24:** 2898–2916

Clough SJ, Bent AF (1998) Floral dip: a simplified method for Agrobacterium-mediated transformation of Arabidopsis thaliana. Plant J **16:** 735–743

Dhawan R, Luo H, Foerster AM, Abuqamar S, Du HN, Briggs SD, Mittelsten Scheid O, Mengiste T (2009) HISTONE MONOUBIQUITINATION1 interacts with a subunit of the mediator complex and regulates defense against necrotrophic fungal pathogens in *Arabidopsis*. Plant Cell **21:** 1000–1019

Elfving N, Davoine C, Benlloch R, Blomberg J, Brännström K, Müller D, Nilsson A, Ulfstedt M, Ronne H, Wingsle G, et al (2011) The Arabidopsis thaliana Med25 mediator subunit integrates environmental cues to control plant development. Proc Natl Acad Sci USA **108:** 8245–8250

Geng F, Tansey WP (2012) Similar temporal and spatial recruitment of native 19S and 20S proteasome subunits to transcriptionally active chromatin. Proc Natl Acad Sci USA **109:** 6060–6065

Geng F, Wenzel S, Tansey WP (2012) Ubiquitin and proteasomes in transcription. Annu Rev Biochem **81:** 177–201

Gillmor CS, Park MY, Smith MR, Pepitone R, Kerstetter RA, Poethig RS (2010) The MED12-MED13 module of Mediator regulates the timing of embryo patterning in Arabidopsis. Development **137:** 113–122

Imura Y, Kobayashi Y, Yamamoto S, Furutani M, Tasaka M, Abe M, Araki T (2012) CRYPTIC PRECOCIOUS/MED12 is a novel flowering regulator with multiple target steps in Arabidopsis. Plant Cell Physiol **53:** 287–303

Iñigo S, Alvarez MJ, Strasser B, Califano A, Cerdán PD (2012) PFT1, the MED25 subunit of the plant Mediator complex, promotes flowering through CONSTANS dependent and independent mechanisms in Arabidopsis. Plant J **69:** 601–612

Ito J, Sono T, Tasaka M, Furutani M (2011) MACCHI-BOU 2 is required for early embryo patterning and cotyledon organogenesis in Arabidopsis. Plant Cell Physiol **52:** 539–552

Kidd BN, Edgar CI, Kumar KK, Aitken EA, Schenk PM, Manners JM, Kazan K (2009) The mediator complex subunit PFT1 is a key regulator of jasmonate-dependent defense in *Arabidopsis*. Plant Cell **21:** 2237–2252

Kim YJ, Zheng B, Yu Y, Won SY, Mo B, Chen X (2011) The role of Mediator in small and long noncoding RNA production in Arabidopsis thaliana. EMBO J **30:** 814–822

Klose C, Buche C, Fernandez AP, Schafer E, Zwick E, Kretsch T (2012) The Mediator complex subunit PFT1 interferes with COP1 and HY5 in the regulation of Arabidopsis light signaling. Plant Physiol **160:** 289–307

Knight H, Thomson AJ, McWatters HG (2008) SENSITIVE TO FREEZING6 integrates cellular and environmental inputs to the plant circadian clock. Plant Physiol **148:** 293–303

Kraft E, Stone SL, Ma L, Su N, Gao Y, Lau OS, Deng XW, Callis J (2005) Genome analysis and functional characterization of the E2 and RING-type E3 ligase ubiquitination enzymes of Arabidopsis. Plant Physiol **139:** 1597–1611

Lalanne E, Michaelidis C, Moore JM, Gagliano W, Johnson A, Patel R, Howden R, Vielle-Calzada JP, Grossniklaus U, Twell D (2004) Analysis of transposon insertion mutants highlights the diversity of mechanisms underlying male progamic development in Arabidopsis. Genetics **167:** 1975–1986

Lee HK, Park UH, Kim EJ, Um SJ (2007) MED25 is distinct from TRAP220/MED1 in cooperating with CBP for retinoid receptor activation. EMBO J **26:** 3545–3557

Lipford JR, Smith GT, Chi Y, Deshaies RJ (2005) A putative stimulatory role for activator turnover in gene expression. Nature **438:** 113–116

Lowry OH, Rosebrough NJ, Lewis Farr A, Randall RJ (1951) Protein measurement with the Folin phenol reagent. J Biol Chem **193:** 265–275

Mathur S, Vyas S, Kapoor S, Tyagi AK (2011) The Mediator complex in plants: structure, phylogeny, and expression profiling of representative genes in a dicot (Arabidopsis) and a monocot (rice) during reproduction and abiotic stress. Plant Physiol **157:** 1609–1627

McElver J, Tzafrir I, Aux G, Rogers R, Ashby C, Smith K, Thomas C, Schetter A, Zhou Q, Cushman MA, et al (2001) Insertional mutagenesis of genes required for seed development in Arabidopsis thaliana. Genetics **159:** 1751–1763

Milbradt AG, Kulkarni M, Yi T, Takeuchi K, Sun ZY, Luna RE, Selenko P, Näär AM, Wagner G (2011) Structure of the VP16 transactivator target in the Mediator. Nat Struct Mol Biol **18:** 410–415

Muratani M, Kung C, Shokat KM, Tansey WP (2005) The F box protein Dsg1/Mdm30 is a transcriptional coactivator that stimulates Gal4 turnover and cotranscriptional mRNA processing. Cell **120:** 887–899

Myung J, Kim KB, Crews CM (2001) The ubiquitin-proteasome pathway and proteasome inhibitors. Med Res Rev **21:** 245–273

Nakamura Y, Yamamoto K, He X, Otsuki B, Kim Y, Murao H, Soeda T, Tsumaki N, Deng JM, Zhang Z, et al (2011) Wwp2 is essential for palatogenesis mediated by the interaction between Sox9 and mediator subunit 25. Nat Commun **2:** 251

Ossowski S, Schwab R, Weigel D (2008) Gene silencing in plants using artificial microRNAs and other small RNAs. Plant J **53:** 674–690

Ou B, Yin KQ, Liu SN, Yang Y, Gu T, Wing Hui JM, Zhang L, Miao J, Kondou Y, Matsui M, et al (2011) A high-throughput screening system for Arabidopsis transcription factors and its application to Med25-dependent transcriptional regulation. Mol Plant **4:** 546–555

Peng M, Hannam C, Gu H, Bi YM, Rothstein SJ (2007) A mutation in NLA, which encodes a RING-type ubiquitin ligase, disrupts the adaptability of Arabidopsis to nitrogen limitation. Plant J **50:** 320–337

Rana R, Surapureddi S, Kam W, Ferguson S, Goldstein JA (2011) Med25 is required for RNA polymerase II recruitment to specific promoters, thus regulating xenobiotic and lipid metabolism in human liver. Mol Cell Biol **31:** 466–481

Rosso MG, Li Y, Strizhov N, Reiss B, Dekker K, Weisshaar B (2003) An Arabidopsis thaliana T-DNA mutagenized population (GABI-Kat) for flanking sequence tag-based reverse genetics. Plant Mol Biol **53:** 247–259

Rotin D, Kumar S (2009) Physiological functions of the HECT family of ubiquitin ligases. Nat Rev Mol Cell Biol **10:** 398–409

Roupelieva M, Griffiths SJ, Kremmer E, Meisterernst M, Viejo-Borbolla A, Schulz T, Haas J (2010) Kaposi's sarcoma-associated herpesvirus Lana-1 is a major activator of the serum response element and mitogen-activated protein kinase pathways via interactions with the Mediator complex. J Gen Virol **91:** 1138–1149

Salghetti SE, Caudy AA, Chenoweth JG, Tansey WP (2001) Regulation of transcriptional activation domain function by ubiquitin. Science **293:** 1651–1653

Salghetti SE, Muratani M, Wijnen H, Futcher B, Tansey WP (2000) Functional overlap of sequences that activate transcription and signal ubiquitin-mediated proteolysis. Proc Natl Acad Sci USA **97:** 3118–3123

Santner A, Estelle M (2010) The ubiquitin-proteasome system regulates plant hormone signaling. Plant J **61:** 1029–1040

Stone SL, Hauksdóttir H, Troy A, Herschleb J, Kraft E, Callis J (2005) Functional analysis of the RING-type ubiquitin ligase family of Arabidopsis. Plant Physiol **137:** 13–30

Taatjes DJ (2010) The human Mediator complex: a versatile, genome-wide regulator of transcription. Trends Biochem Sci **35:** 315–322

Tsai CJ, Nussinov R (2011) Gene-specific transcription activation via long-range allosteric shape-shifting. Biochem J **439:** 15–25

Voinnet O, Rivas S, Mestre P, Baulcombe D (2003) An enhanced transient expression system in plants based on suppression of gene silencing by the p19 protein of tomato bushy stunt virus. Plant J **33:** 949–956

Vojnic E, Mourão A, Seizl M, Simon B, Wenzeck L, Larivière L, Baumli S, Baumgart K, Meisterernst M, Sattler M, et al (2011) Structure and VP16 binding of the Mediator Med25 activator interaction domain. Nat Struct Mol Biol **18:** 404–409

Wang W, Chen X (2004) HUA ENHANCER3 reveals a role for a cyclin-dependent protein kinase in the specification of floral organ identity in Arabidopsis. Development **131:** 3147–3156

Wang X, Muratani M, Tansey WP, Ptashne M (2010) Proteolytic instability and the action of nonclassical transcriptional activators. Curr Biol **20:** 868–871

Wigge PA (2011) FT, a mobile developmental signal in plants. Curr Biol **21:** R374–R378

Wigge PA, Kim MC, Jaeger KE, Busch W, Schmid M, Lohmann JU, Weigel D (2005) Integration of spatial and temporal information during floral induction in Arabidopsis. Science **309:** 1056–1059

Wollenberg AC, Strasser B, Cerdán PD, Amasino RM (2008) Acceleration of flowering during shade avoidance in Arabidopsis alters the balance between FLOWERING LOCUS C-mediated repression and photoperiodic induction of flowering. Plant Physiol **148:** 1681–1694

Xu R, Li Y (2011) Control of final organ size by Mediator complex subunit 25 in Arabidopsis thaliana. Development **138:** 4545–4554

Yang F, DeBeaumont R, Zhou S, Näär AM (2004) The activator-recruited cofactor/Mediator coactivator subunit ARC92 is a functionally important target of the VP16 transcriptional activator. Proc Natl Acad Sci USA **101:** 2339–2344

Yang M, Hay J, Ruyechan WT (2008) Varicella-zoster virus IE62 protein utilizes the human mediator complex in promoter activation. J Virol **82:** 12154–12163